Differential Model EMI Filter Analysis for Interleaved Boost PFC Converters Considering Optimal Phase Shifting

Esfetanaj, Naser Nourani; saad, Yamen ; Ahmad Sakaria, Omar ; Wang, Huai; Davari, Pooya

Published in:
2020 22nd European Conference on Power Electronics and Applications (EPE'20 ECCE Europe)

DOI (link to publication from Publisher):
10.23919/EPE20ECCEEurope43536.2020.9215730

Publication date:
2020

Document Version
Version created as part of publication process; publisher's layout; not normally made publicly available

Differential Model EMI Filter Analysis for Interleaved Boost PFC Converters Considering Optimal Phase Shifting

Naser Nourani Esfetanaj
Department of Energy Technology, Aalborg University
Aalborg, Denmark
nne@et.aau.dk

Yamen Saad
Converdan A/S,
Rødding, Denmark
ys@converdan.com

Omar Ahmed Sakaria, Huai Wang, Pooya Davari
Department of Energy Technology, Aalborg University
Aalborg, Denmark
soah17@student.aau.dk,
hwa@et.aau.dk,
pda@et.aau.dk

Keywords

« DM EMI Filter analysis », « Interleaved PFC Converters », « phase-shifting ».

Abstract

Interleaved Power Factor Correction (PFC) has become a most popular topology from efficiency and power density point of view over single-switch boost PFC. The dependency of the Differential Model (DM) Electromagnetic Interference (EMI) noise magnitude on input current ripple leads to investigate the influence of the interleaved technique on EMI noise. Hence, this paper provides a comprehensive investigation for the design of DM EMI filter a single-phase interleaved PFC targeting to minimize component size. It is shown how different operation modes (continuous and discontinuous conduction mode) and switching frequency may influence the required filter attenuation and, consequently, the EMI filter size. Furthermore, the impact of the number of interleaved stages and optimal phase shifting on the required filter attenuation is analyzed. Finally, the influence of optimal phase shifting achieve an overall minimum EMI filter corner frequency is discussed. Experimental results from a 2 kW interleaved single-phase boost PFC converter validate the effectiveness of the proposed optimal phase shifting method.

Introduction

Complying harmonic standards and power factor of the input AC power led to the development of boost power factor correction (PFC) circuits to achieve a power factor close to unity. Moreover, using interleaving PFC has many advantages for instance increase power densities, reducing the overall volume of the design, and reduce RMS current in the boost capacitor. Furthermore, the use of the interleaved configuration, which is shown in Fig.1, brings a significant reduction in the switching frequency ripple component due to the ripple cancelation effect [1]. Notably, ensuring sinusoidally shaped input currents in connection with DM EMI input filters, which are limiting high-frequency noise from being transmitted from the converter to the grid [2]. However, high penetration of power electronics converter in the grid causes some challenging EMI issues due to inherent pulse energy conversion characteristics. Thereby, these unintended emissions must be limited to fulfill noise emission standards, such as CISPR 11 for frequencies beyond 150kHz [3]. Whereby, due to the increasing demand of the pulse-width modulated (PWM) converters, some standards are defined under 150 kHz in some application instance, CISPR 14 (Induction hobs) [4], and CISPR 15 (Lighting equipment) [5]. Further, it is accepted that the decreased input ripple current reduces the DM EMI noise magnitude and filter requirement attenuation which makes the DM EMI filter size smaller and corner frequency higher [1]. Furthermore, the EMI filter is one of the effective methods for damping EMI noise emission. From the EMI perspective view, finding the optimal phase shift angles which give the optimal corner frequency is a big challenge. Hence, designing optimal DM EMI filters for interleaved boost PFC applications can be considerably challenging, especially in low-frequency EMI range between 2-150kHz. This paper investigates the effect of phase-shift and number of interleaved stages in a single-phase PFC on DM EMI filter sizing. It is shown that an optimal phase-shift angle can be found depending on the power converter selected switching frequency, number of interleaved stages and its mode of operation which can minimize the EM filter size. Moreover, in order to highlight the importance of phase-shift control

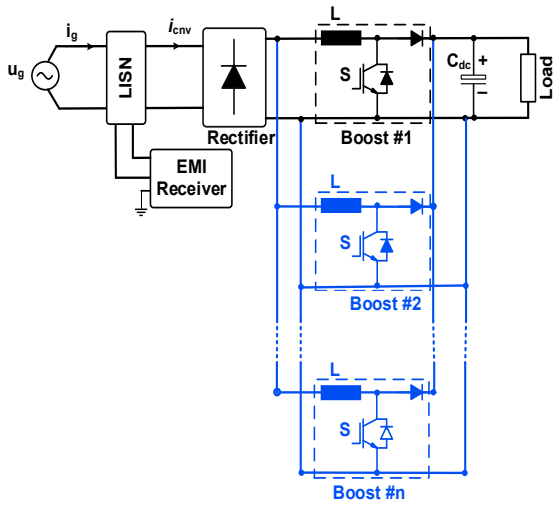

Fig. 1: Topology of Interleaved boost PFC converter with including LISN and EMI receiver.

in different applications, the studies are carried out for both below and above 150 kHz frequency ranges of standard requirements.

This paper is organized as follows. Section II shows the designing process for the two-step EMI filter. Further, it describes the EMI measurement setup according to the CISPR standard, including line impedance stabilizing network (LISN) and EMI receiver. Section III presents to design optimal DM EMI filter for interleaved boost PFC due to finding the optimal filter corner frequencies with considering two-step EMI filters in Band A and B. Subsequently, the benefit of optimal phase shifting in interleaved units will be developed, where it will be shown that the amount of filter attenuation decreasing. Section IV illustrates the experimental results achieved for the two interleaved boost PFC converter by presenting the standard or optimal phase shift. Finally, conclusions are drawn in Section V.

EMI Simulation

DM Filter Design

The EMI filter is used to protect the utility from the high frequency conducted emissions noise, which should comply with EMI standards requirements, more details about the emission standard are discussed before. Therefore, the design of a two-stage filter structure, as shown in Fig. 2, is considered in the following. Further, the primary purpose of the EMI filter is damping emission noise and make it lower than limits to fulfill the standards limit. Furthermore, the selecting filter component is depending on the required filter attenuation Att_{req}, which can be calculated from

$$A_{tt_{req}}(f)[dB] = U_{\max}(f)[dB\mu V] - CISPR_{\lim it}(f)[dB\mu V] + M \arg in[dB] \quad (1)$$

Where, U_{max} is the maximum peak of the spectrum which can measurement based on the PLECS simulation and plotting based on the (4); Att_{req} is the quantity of noise that filters should be damping it. $CISPR_{limit}$ can be found from the standard requirements, which is shown in Fig. 3. Moreover, the filter designing margin is considered 6 dB due to component degradation and EMI parameter tolerance. Hence, two-step EMI filter including inductor and capacitor size can be found as [6]

$$A_{tt_{req}}(f) = \left|((j2\pi f)^2.L_{DM}.C_{DM} + 1)^2 + (2\pi f)^2.L_{DM}.C_{DM}\right| \quad (2)$$

As discussed before, the reduce the input ripple current can be effect on the DM EMI noise magnitude (U_{max}), which will make the DM filter smaller. In addition, the dependency of EMI filter corner frequency to filter component, lead a challenge in selecting filter component size. Hence, lowering the EMI filter component size makes the DM filter corner frequency higher. Whereby, the filter corner frequency can be found from

$$fc = \frac{1}{2.\pi\sqrt{L_{DM}C_{DM}}} \quad (3)$$

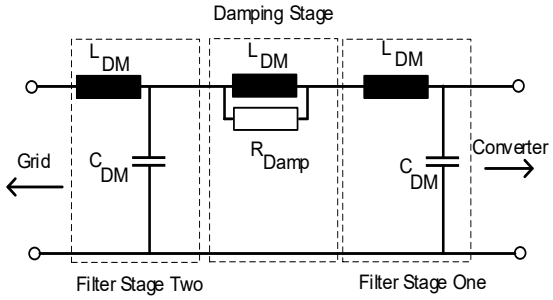

Fig. 2: Two stages DM EMI filter configuration.

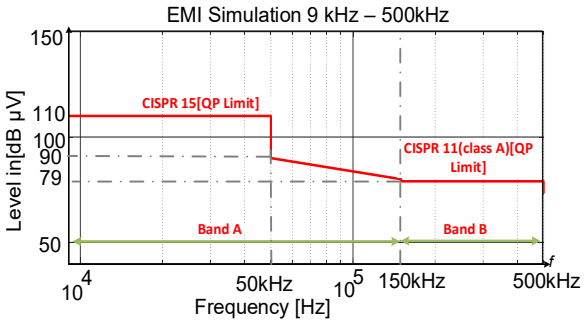

Fig. 3: Considered emission limits following CISPR 15 [5] and CISPR 11 [3] based on QP (Quasi Peak). Band B is only shown up to 500 kHz.

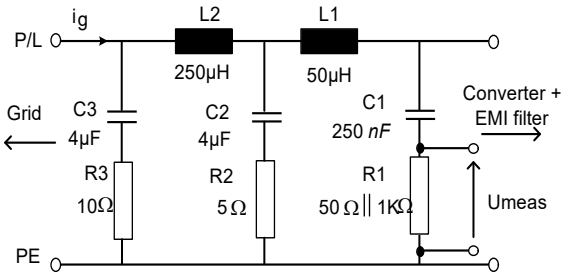

a)

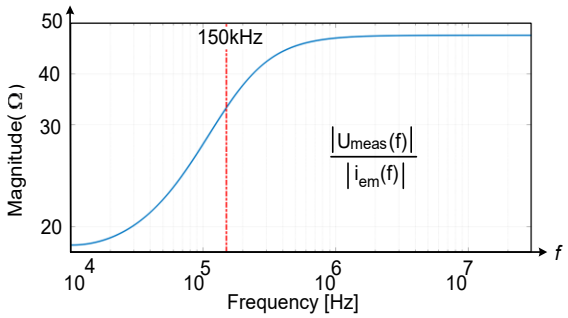

b)

Fig. 4. LISN recommendation from CISPR 16 for band A, (a) per-phase circuit diagram, (b) per-phase DM mode transfer function [6]-[7].

LISN and EMI Receiver

A LISN is specified for EMI tests according to CISPR 16[8], to guarantee the repeatable of the measurements. Moreover, LISN, not only provides the decoupling line from the device under test (DUT) but also provides an interface between the DUT and the test receiver. The structure of the LISN for using in 9kHz-30MHz is shown in Fig 4. Notably, LISN can measure an RMS time-domain voltage (u_{meas}) to define EMI noise based on the (4). Hence, the EMI test receiver used QP detection for detecting EMI peak measurement. Moreover, Bandwidth of the 4th order Butterworth bandpass filter for band A(9-150kHz) is 200Hz, and for band B(150kHz-30MHz) is 9kHz. Finally, with considering of (4), EMI peak measurement [7]-[9] can be estimated, by

$$U_{\max}[dB\mu V] = 20\log[1/\mu V \sum_{f=MB-\frac{BW}{2}}^{f=MB+\frac{BW}{2}} u_{meas}(f)\cdot RBW(f)] \quad (4)$$

Investigation of EMI Filter Design

Non-Interleaving Single Unit

In this part, EMI filter design for non-interleaving 1-unit PFC, which is shown with black color in Fig. 1, is studied. The boost-inductor design for continuous conduction mode (CCM) [10]-[11], and discontinuous conduction mode (DCM) [12] operation has already been presented in the literature. Hence, for the sake of simplicity, only the most well-known equations will be specified in this section. Notably, depending on the inductor current, the boost PFC converter can operate in different modes, including CCM and DCM. Hence, designing an EMI filter to fulfill the standard requirements, for both scenarios is different due to different currents ripple. Furthermore, Inductor current for CCM and DCM operations can be calculated respectively from

$$L_{CCM} = \frac{u_o}{4.\Delta i_{L,\max}.f_{sw}} \quad (5)$$

$$L_{DCM} = \frac{u_g^2.(1-\frac{u_g}{u_o})}{4.\Delta i_{L,\max}.f_{sw}} \quad (6)$$

Parameter values for single-phase PFC in order to finding filter required attenuation with respect to different frequency switching in CCM and DCM as u_o = 400 V, u_g = 230√2 V, P_{max} = 1000 W, $\Delta i_{L,max}$ = 0.62 A. Hence, inductor sizes are can be calculated from (5) and (6) for the different case studies. So, inductor size for CCM and DCM mode are presented at table I. It is clear that the size of the inductor for DCM mode is lower than CCM mode. Whereby the maximum peak of the spectrum (U_{max}) for different frequency switching can be found based on the PLECS simulation and (4). Therefore, the EMI filter component (L_{DM} C_{DM}) and corner frequency can be achieved from (2) and (3), respectively. In the following, Fig. 5(a) and Fig 5(c) shows the Att_{req} requirement to design a DM two-stage EMI filter based on the (1) in different switching frequency. So, Fig. 5(b) and Fig 5(d) exposes the filter corner frequency (f_c) with considering different switching frequency for two stages DM EMI filter in band A and B based on the (1)-(2). It is clear from Fig. 5(a) and Fig. 5(b), Att_{req} increases significantly at f_{sw} = 50 kHz because the standard limit (CISPR 15) gets more restricted beyond = 50 kHz for band A which is shown from Fig. 3. Furthermore, it is generally known that CCM has the lower current ripple in comparison to DCM modes. Therefore, as a consequence of Fig.5(a) and (d), under CCM operation lower attenuation (Att_{req}) is required. One can see that, due to the first noise peak will be appeared at the switching frequency f_{sw} in band A, the best f_{sw} selection is to be higher than 150 kHz. But if f_{sw} has to be less than 150 kHz,

Table I: Inductor size value for single phase unite in DCM and CCM mode based on the (5) and (6).

		Switching Frequency(kHz)											
	20	25	30	35	37.5	45	50	70	75	140	150	250	500
CCM (mH)	8.06	6.45	5.38	4.61	4.30	3.58	3.23	2.3	2.15	1.15	1.08	0.65	0.32
DCM (µH)	247	197.6	164.7	141.1	131.7	109.8	98.8	70.6	65.8	35.3	32.9	19.7	9.8

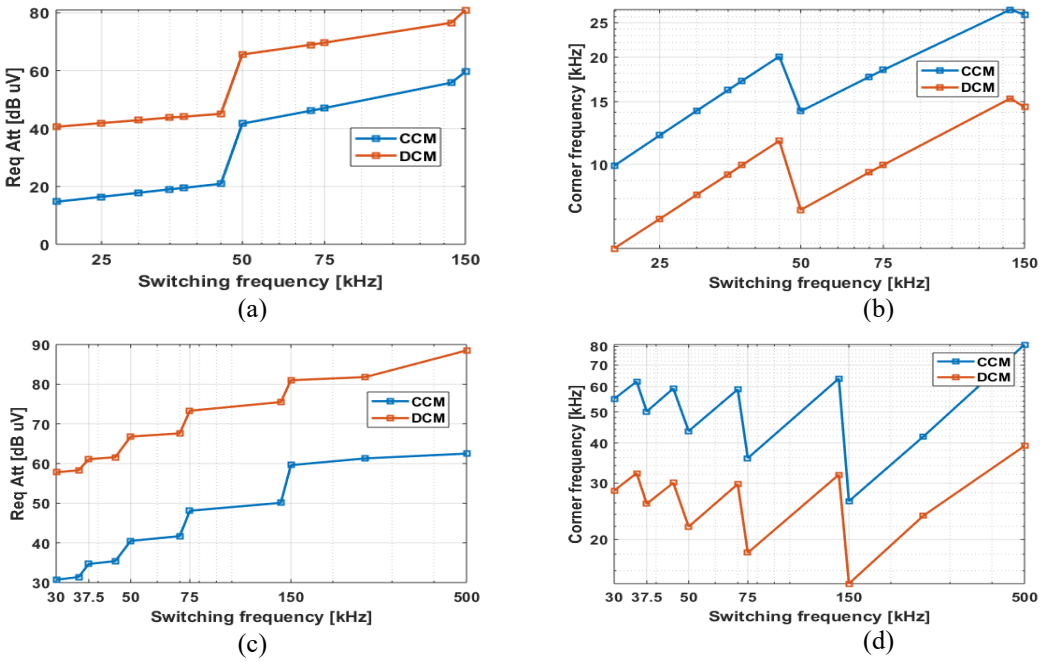

Fig. 5: The relation between the required attenuation and the switching frequency in a) Band A. c) B B base on the (1) for single converter unit. The relation between the two-stage filter corner frequency the switching frequency in b) Band A, d) Band B base on the (1)-(2).

therefore, two or higher stages filter should use to damp attenuation requirement. As it is clear that from the Fig. 5(a), selecting the switching frequency under the 50 kHz is need to low filter requirement attenuation in comparison with selecting above then 50kHz. Moreover, the first noise peak which appears in band B is the kth multiple of the switching frequency f_{sw}. Notably, it clear that from Fig. 5(c) that, the filter corner frequency f_c is significantly decreased at the divisors of f_{sw} = 150 kHz (30, 37.5, 50 ...150 kHz). As a result, the main reason for that is choosing the switching frequency to appear first noise peak f_D higher than 150 kHz in-band B. For instance, choosing f_{sw} = 75 kHz, the first noise peak appears at 150 kHz which is the second harmonics of f_{sw} = 75 kHz. Moreover, if f_{sw} is chosen 70 kHz, the first noise peak appears at f_{sw} = 210 kHz which is the third harmonics of f_{sw} = 70 kHz. Hence, the first peak above 150kHz for the case with f_{sw} = 70 kHz is the lower magnitude and higher frequency in comparison to the second case with f_{sw} = 75 kHz. Whereby, it is not efficient to switch at the previously mentioned critical frequencies and use a switching frequency just a bit lower than them, which will increase the filter corner frequency without affecting the boost inductor size.

Interleaving Using Standard Phase-Shift

The interleaved boost PFC and the beneficiary have been previously introduced in the literature [1]. In this section, the interleaving technique to achieve optimal design DM EMI filter has been studied. Hence, up to four interleaved units have been run at different switching frequencies in band A and band B, to achieve the connection between required attenuation with interleaving and optimal phase shift. Notably, the typical phase shift $360°/N$ (N is the number of the interleaved converter) is used here between the interleaved units. As discussed before, the inductor size for interleaved will be $L_1 = NL$ due to ensure constant energy storage. As previously mentioned, in band A, the first noise peak will appear at the switching frequency f_{sw}. By interleaving, the equivalent switching frequency will be N f_{sw}, where N is the number of the interleaved units. For example, in two units interleaved at f_{sw} = 25 kHz, the equivalent switching frequency will be 50 kHz. Interleaved technique can be the decreased ripple current, and $K_C(d)$ is defined as a cancellation factor, which is the ratio between the input current ripple after interleaving and the inductor current ripple in Non-interleaving one unit:

$$K_c(d) = \frac{N.(d - \frac{m}{N}).(\frac{m+1}{N} - d)}{d.(1-d)} \tag{7}$$

Where N is the number of the interleaved units, $m=floor\ (N.d)$ and, d is the duty cycle. More information about the effect of interleaving on ripple current has been presented on [1]. Fig. 6(a) is shown the connection between the required attenuation and the switching frequency up to four units for CCM mode in Band A. It can be seen in Fig. 6(b) and 6(d) that there is a drop in the filter corner frequency at f_{sw} = 50 kHz and f_{sw} = 25 kHz for one and two units, respectively. Since the equivalent switching frequency is $N\ f_{sw}$, then there is no need to use a filter if the switching frequency higher than 75 kHz in two units, 50 kHz in three units, and 37.5 kHz in four units because there will be no peak noise in Band A. The EMI filter component values and corner frequency can be achieved from (2) and (3), respectively. So, Fig. 6(b) shows the filter corner frequency (f_c) with considering different switching frequencies for two stages DM EMI filter in band A based on the (1)-(2). Moreover, Fig. 7 shows the EMI simulation at f_{sw} = 35 kHz in non-interleaving (one unit), and in two units interleaved (180^o phase shifting). As it is clear that, the first noise peak is appeared at f_{sw} = 70 kHz after interleaving while it is at f_{sw} = 35 kHz before interleaving. Notably, in two units interleaved, the odd order of the switching frequency harmonics is canceled out, while it does not affect the even harmonics. Hence, according to Fig. 6(d), the filter corner frequency is increasing at a specific switching frequency range (30-37.5kHz, 50-75kHz, and > 150 kHz) in two units interleaved. In addition, for one unit (non-interleaved), the first noise peak beyond 150 kHz will be the odd order of the switching frequency harmonics at those ranges. Hence, interleaving two units will be eliminated odd-order mention noise. As a consequence, then the filter will be designed based on the next even harmonics, which has a higher frequency and lower amplitude, as can be illustrated in Fig. 6(c), where the required attenuation is lower in those ranges. For instance, if f_{sw} = 35 kHz, the first noise peak in one unit (non-interleaved) in-band B will be at f_{sw} = 175 kHz, which is the 5th harmonic. But by considering interleaving two units with 180^o as phase shift, the noise peak will

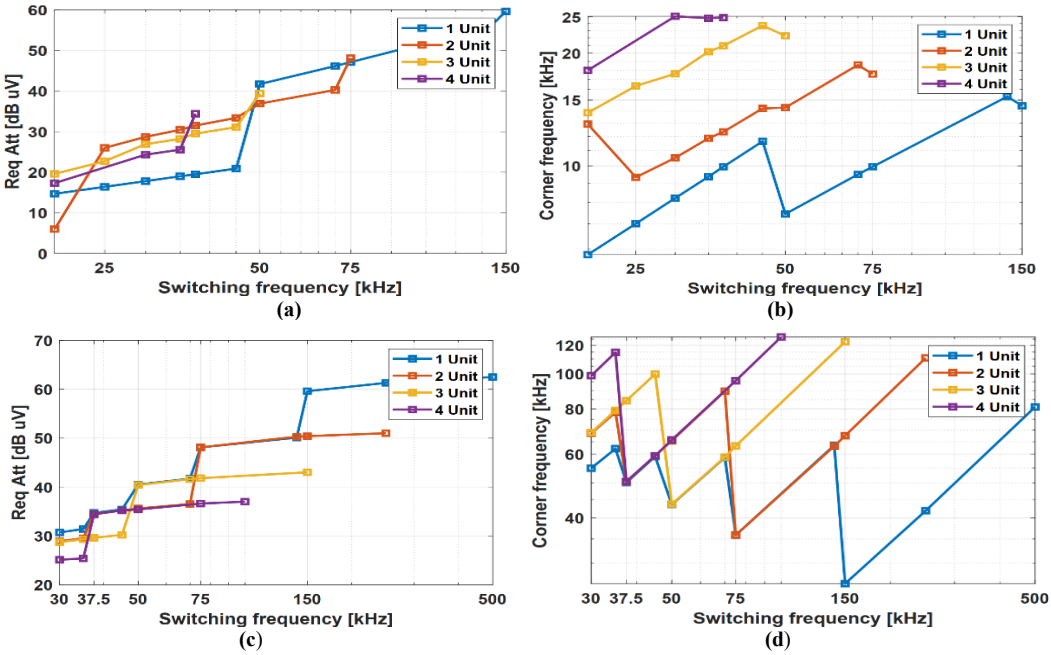

Fig. 6: The relation between the required attenuation and the switching frequency up to four units interleaved in a) Band A. c) Band B. The relation between the 2-stages filter corner frequency and switching frequency up to four units interleaved in b) Band A d) Band B for CCM based on the required attenuation (1)-(2). The typical phase shift is considered 360°/ N.

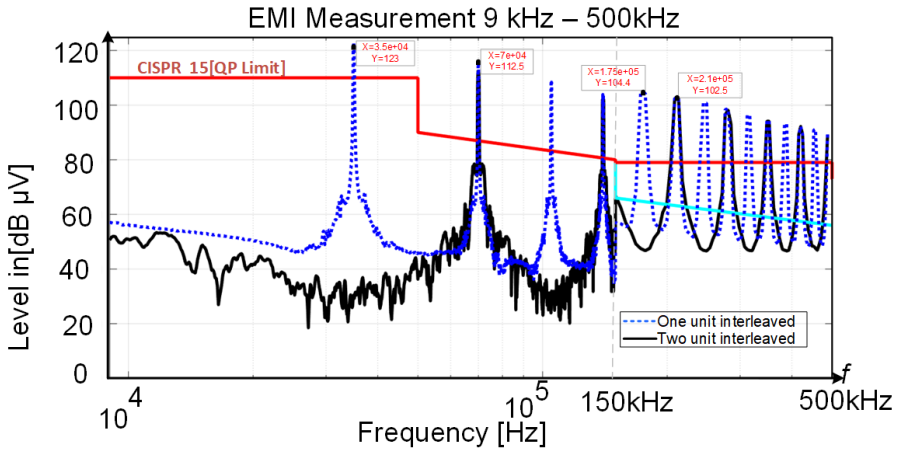

Fig. 7: EMI simulation approach for one and two-unit interleaved CCM at f_{sw} = 35 kHz based on PLECS software (interleaved typical phase shift is equal 180°).

have happened at f_{sw} = 210 kHz (6th harmonic), which is shown in Fig. 7 shows. Therefore, the filter size decreases due to it happened at a high frequency.

Interleaving Using Optimal Phase-Shift

The conventional interleaving with typical phase-shift does not give any beneficiary at some switching frequency ranges like 75-150 kHz in band B, which is clear that form Fig.6(c). Hence, to target the cancellation effect to occur at any order of harmonics, a different phase-shift angle will be presented in this section. Hence, Fig. 8(a) and Fig.8(b) are given an optimal phase-shift effect on required attenuation, and filter corner frequency in different switching frequencies on two unites Interleaved, respectively. As it is visible that the required attenuation and filter corner frequency are the same for one unit non-interleaved and two units with a standard phase shift between 75-150 kHz frequency range. Notably, using optimal phase shifting is can be provided a beneficiary instance decreasing required attenuation

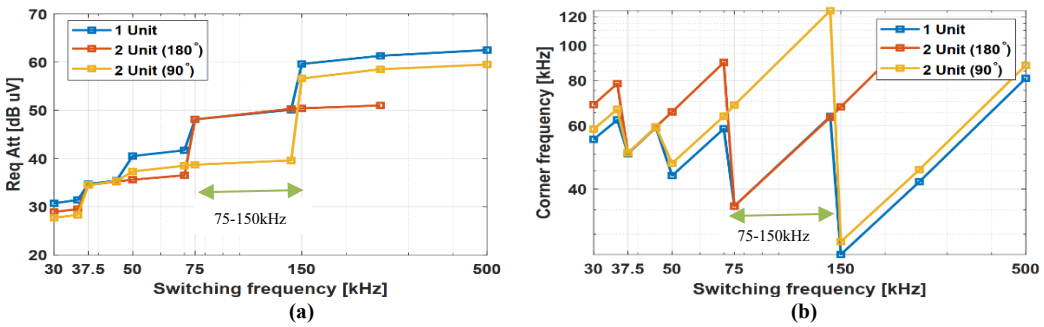

Fig. 8: Choice different phase shift angle for two units interleaved in Band B for CCM mode, a) The relation between the required attenuation with the switching frequency, b) The relation between the filter corner frequency with the switching frequency.

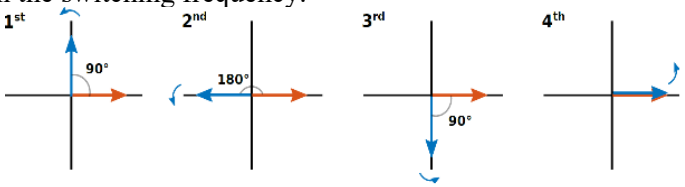

Fig. 9: Noise phasor diagram for two units interleaved with 90° phase shift.

and increasing corner frequency for using Interleaving technique on switching frequency range 75-150kHz. Because of optimal phase shifting can eliminate the second-order harmonics of the switching frequency, which is the first noise will appear above then 150kHz if the switching frequency is choice at the range (75kHz- 150kHz). Notably, Fig. 9 shows the noise phasor diagram for two units interleaved with a 90° phase shift. As can be found on the 2nd, the total noise will be zero due to the noise phase cancelation of two units.

$$\theta = \frac{360^o}{N} \quad if\ k\ not\ a\ multiple\ of\ N \tag{8}$$

$$\theta = \frac{360^o}{\min(floor(N.k))} \quad if\ k\ a\ multiple\ of\ N \tag{9}$$

Where k is the harmonic order of the frequency switching, which will be appeared as a first noise peak in Band B. In addition, the resulting of optimal phase shift angle, found by calculations according to (8) and (9) are summarized in Table II. Whereby, two simulation cases are examined to confirm the optimal phase shift, especially in band B with different phase-shifting (180° and 45°). In the following, Fig. 10 illustrates obtained comparative results with the proposed optimal phase shift with and without EMI filters f_{sw} = 20 kHz. Hence, Table III summarizes the outcomes of two simulation case study, including required attenuation and corner frequency. Notably, a 45° phase shift in comparison of 180° is needed lower filter attenuation in the band B while 180° need to high filter attenuation.

Table II: Optimal phase shift angles at the switching frequency range (30-150kHz) up to four units interleaved based on the (8) and (9).

Frequency	30kHz	37.5kHz	50kHz	75kHz	150kHz
Harm. order:	5^{th}	4^{th}	3^{th}	2^{th}	1^{th}
2 Units	**180°**	45°	**180°**	90°	**180°**
3 Units	**120°**	**120°**	40°	**120°**	**120°**
4 Units	**90°**	45°	**90°**	90°	**90°**

Table III: Band B EMI filter design based on PLECS software for standard (180°) and optimal phase shift(45°) base on the (8) and (9).

Phase	Δi_L	L(mH)	f_D[kHz]	Attreq[dB]	L_{DM} (µH)	C_{DM} (nF)
180°	2.6	1	33.2	52.3	180	**127**
45°	2.6	1	43	43.5	180	**76**

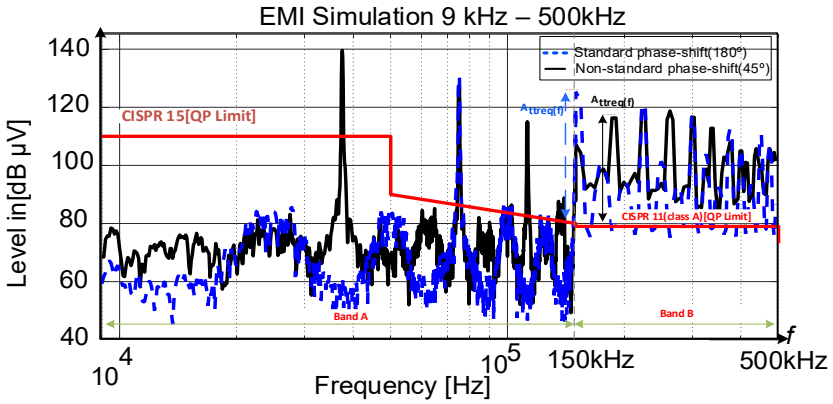

a) Without EMI filter

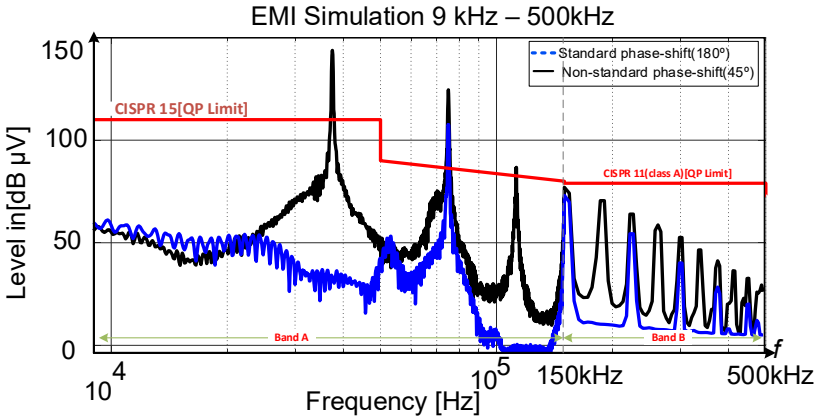

b) With EMI filter

Fig. 10: EMI simulation approach for two-unit interleaved CCM at f_{sw} = 37.5 kHz based on PLECS software for standard (180°) and optimal phase shift (45°) base on the (8) and (9).

Experimental Results

To evaluate the previously done examinations, the two-unit Interleaved boost PFC rectifier shown in Fig. 1 is considered under CCM, as it is summarized in Table IV. A laboratory setup including EMI receiver and LISN and the two-unit interleaved converter provides simulation verification. Moreover, the simulation model has been run in PLECS software. The sampling frequency of simulation and experimental results is 100 kHz. Whereby, Fig. 11 is measured experimental waveform of two units -

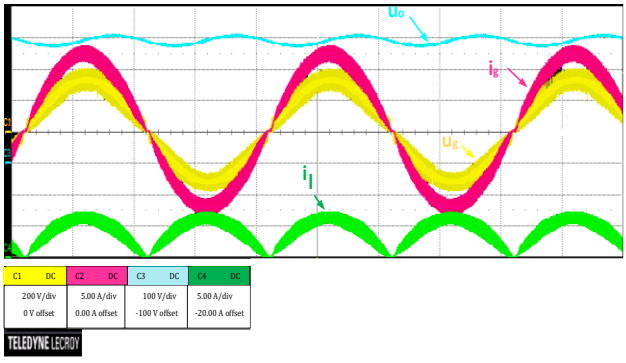

Fig.11 Measured experimental waveform of two units interleaved with Table IV parameters (f_{sw} = 20 kHz) and phase shift 90°

Table IV: Case study specification

Grid Voltage	u_g	230 V
Output Voltage	U_o	400 V
Output Power	P_o	2 kW
Fundamental Frequency	f_o	50 Hz
DC Link Inductor	L	1.8mH
DC-Link Capacitor	C	500 µF
Switching Frequency	f_{sw}	20 kHz
Capacitor Ripple	dV_{dcmax}	20 V
Inductor Ripple	di_{lmax}	20 A
Phase Shift	degree	0°, 90°, 180°

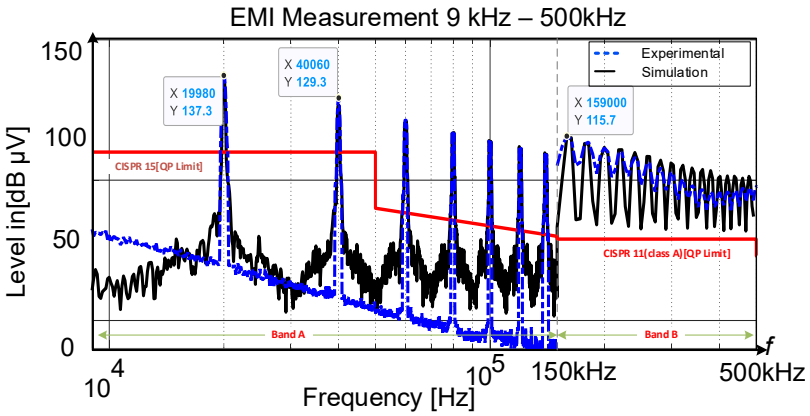

(a) α=0

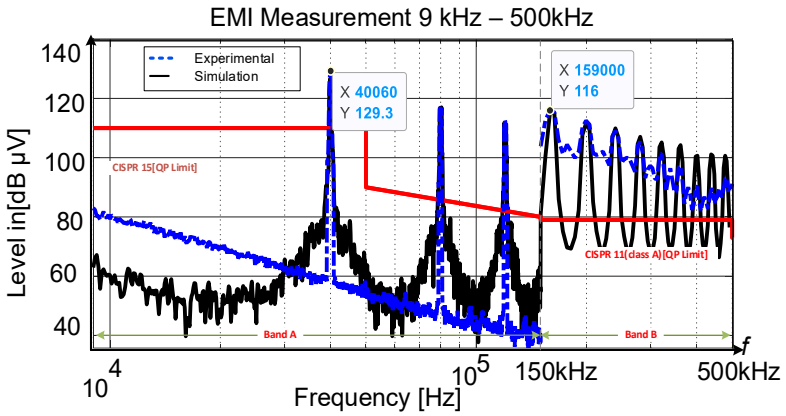

(b) α=180 (conventional)

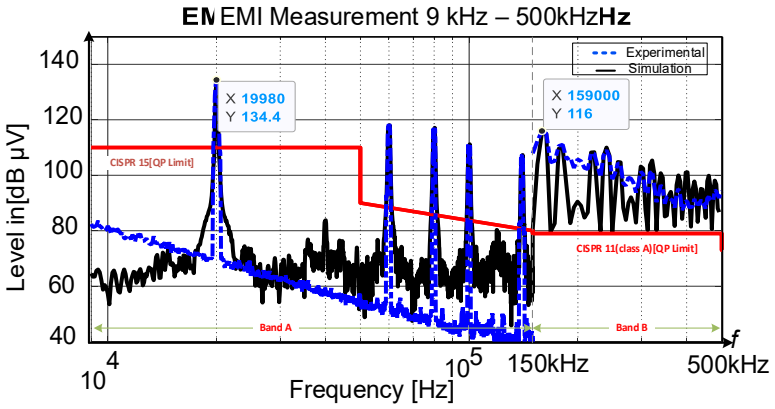

(c) α=90 (non-conventional)

Fig. 12: Obtained EMI measurement for 2-unit Interleaved Boost PFC converter, simulation-based PLECS software, and experimental measurement. Test system specification is based on the Table (IV).

interleaved with Table IV parameters (f_{sw} = 20 kHz) and phase shift 90°. Moreover, the first test case is two-unit interleaved with phase shift a = 0° and this the same as using 1-unit (Non-interleaved), but the difference is that total boost inductor will be two times of non- interleaving. Hence, Fig.12(a) illustrates the simulation and experimental results for two-unit interleaved without EMI filter and phase shift α = 0°. In the next step, the second test has a 180-degree phase difference between two Interleave PFC, which call conventional interleave (standard phase shift). It is clear from Fig.12 (b), the experimental outcome is validated simulation by considering the standard phase shift between the units. Notably, the first order of harmonics appears in $2f_{sw}$ in comparison with α = 180° in higher frequency.

Notably, Fig.12(c) is shown the optimal phase shift effects with considering 90° as a phase shift between the units for two-unit interleaved without EMI filter. It is clear that the second-order harmonics is disappeared with considering 90° as a phase shift based on the Fig.9. Hence, it can be used to optimize the filter size in band A. As a consequence, the results are shown the selecting optimal phase shift can be canceled selective harmonics, which is essential in calculating required attenuation in filter designing. Since the noise-emission level is above the standard requirement, which is shown in Fig. 12, designing a proper EMI filter is necessary.

Conclusion

This paper investigates the effect of optimal phase-shift selection on EMI filter optimization for both Band A (9-150 kHz) and B (>150 kHz). The obtained results show that, in band A, the interleaved configuration provides high benefit, which is the possibility of not using the filter if the switching frequency higher than 75 kHz in two units, 50 kHz in three units, and 37.5 kHz in four units. Furthermore, in-band B, it has been seen that from Fig. 8, using the typical phase-shift between the units is not efficient at all the switching frequency ranges. Therefore, different phase-shift is used to achieve a high corner frequency. Hence, a generic formula to find the phase shift angles which give the optimal corner frequency in interleaved boost PFC has been found in band B, which is a consequence of Fig. 10. In addition, this paper shows the beneficiary of the optimal phase shift in band A, to cancel selective harmonics to optimize required attenuation for EMI filter designing. Finally, the experimental outcome is to validate the standard phase shift and optimal phase shift effects for band A.

References

[1] Chuanyun Wang, Ming Xu, Fred C Lee, EMI study for the interleaved multi-channel PFC". In: 2007 IEEE Power Electronics Specialists Conference, IEEE. 2007, pp. 1336–1342.

[2] T. Nussbaumer, K. Raggl and J. W. Kolar, Design Guidelines for Interleaved Single-Phase Boost PFC Circuits, in IEEE Transactions on Industrial Electronics, vol. 56, no. 7, pp. 2559-2573, July 2009.

[3] C.I.S.P.R, Limits and methods of measurement of Radio-frequency disturbance characteristics of Industrial, scientific and medical equipment-Publication 11,2010.

[4] C.I.S.P.R., Electromagnetic compatibility - Requirements for household appliances, electric tools and similar apparatus - Part 1: Emission, vol. 14. 2016, p. IEC Int. Special Committee on Radio Interference

[5] C.I.S.P.R., Limits and methods of measurement of radio disturbance characteristics of electrical lighting and similar equipment Interference, vol. 15, 2015, IEC Int. Special Committee on Radio Interference.

[6] M. Hartmann, H. Ertl, J. W. Kolar, EMI Filter Design for a 1 MHz, 10 kW Three-Phase/Level PWM Rectifier, IEEE Transactions on Power Electronics, vol. 26, No.4, pp.1192-1204, April 2011.

[7] P. Davari, F. Blaabjerg, E. Hoene, F. Zare,: Improving 9-150 kHz EMI Performance of Single-Phase PFC Rectifier, In: CIPS 2018; 10th International Conference on Integrate.

[8] C.I.S.P.R., Specification for Radio Interference Measuring Apparatus and Measurement Methods, Publication 16, 2015, p. IEC Int. Special Committee on Radio Interference.

[9] N. Nourani Esfetanaj; S. Peyghami; H. Wang; P. Davari, Analytical Modeling of 9-150 kHz EMI in Single-Phase PFC Converter, IECON 2019 - 45th Annual.

[10] M. Kazerani, P. D. Ziogas, and G. Joos,: A novel active current wave shaping technique for solid-state input power factor conditioners," IEEE Trans. Ind. Electron., vol. 38, no. 1, pp. 72–78, Feb. 1991.

[11] P. Davari, F. Zare, A. Abdelhakim,: Active Rectifiers and Their Control, Control of Power Electronic Converters and Systems Vol. 2 2018, pp. 3-52.

[12] L. Ping and K. Yong, "Design and performance of an AC/DC voltage source converter," in Proc. IEEE INTELEC, 2000, pp. 419–423.